Ab initio density-functional study of NO on close-packed transition and noble metal surfaces: I. Molecular adsorption

2006 J. Phys.: Condens. Matter 18 13

(http://iopscience.iop.org/0953-8984/18/1/002)

INSTITUTE OF PHYSICS PUBLISHING JOURNAL OF PHYSICS: CONDENSED MATTER

J. Phys.: Condens. Matter **18** (2006) 13–40 doi:10.1088/0953-8984/18/1/002

Ab initio density-functional study of NO on close-packed transition and noble metal surfaces: I. Molecular adsorption

Marek Gajdoš, Jürgen Hafner and Andreas Eichler

Institut für Materialphysik and Center for Computational Materials Science, Universität Wien, Sensengasse 8/12, A-1090 Wien, Austria

E-mail: juergen.hafner@univie.ac.at

Received 20 July 2005, in final form 4 August 2005
Published 9 December 2005
Online at stacks.iop.org/JPhysCM/18/13

Abstract

Ab initio density-functional calculations have been used to investigate the molecular adsorption of NO on the close-packed surfaces of late transition metals (Co, Ni, Ru, Rh, Pd, Ir, Pt) and noble metals (Cu, Ag, Au). The energetics, geometry, and vibrational properties of the adsorbate–substrate complex have been calculated. With the exception of Ir and Au, adsorption in a hollow-site is always preferred. On Ir(111) the potential-energy surface for NO adsorption is very flat, with a slight preference for a linear on-top geometry. On Au(111), where NO adsorption is only very weak, bridge-adsorption with a strong tilting of the NO molecule relative to the surface normal is predicted. Among the different hollows on a (111) surface preference changes from hcp on Co, Ni, Ru, Rh to fcc on Cu, Pd, Pt, and Ag. However, not only on Ir, but also on Co, Ru, Rh and Pt are the site-dependent differences in the adsorption energies small enough to allow a coexistence of NO adsorbed on different sites. A careful comparison of the calculated vibrational eigenmodes with the available experimental data leads to full agreement between the predicted site preference and the observed NO stretching frequencies. This leads to a redefinition of the characteristic frequency intervals to be used for the site assignment. The trends in the adsorption energies and in the vibrational spectra are compared to those derived from studies of CO adsorption on the same surfaces and discussed in terms of the filling of the d-band of the substrate. In a forthcoming publication, these studies will be extended to NO dissociation on these substrates.

(Some figures in this article are in colour only in the electronic version)

1. Introduction

The nitric oxides, similarly to carbon oxides, belong to the air-pollutants produced by combustion engines. Therefore the necessity to develop efficient catalytic converters for the

post-processing of the exhaust gases has stimulated extensive investigations of the adsorption and decomposition of NO_x molecules on the surfaces of prospective metallic catalysts; for recent reviews see, for example, Over [1] and Brown and King [2]. In order to find the optimal composition of the most effective catalyst, a detailed and quantitative understanding of the adsorption behaviour of CO and of different NO_x species is required. A recent study [3] has been devoted to the investigation of the trends dominating CO adsorption on the close-packed surfaces of the late transition and noble metals, highlighting the successes and limitations of a density-functional theory (DFT) of adsorption. Although NO is of comparable importance from the environmental point of view, the number of studies devoted to NO adsorption is at least one order lower than for CO.

The dissociation energy of NO ($E_{\mathrm{diss}}^{\mathrm{NO}} = 630$ kJ mol^{-1}) [4] is much lower than that of CO ($E_{\mathrm{diss}}^{\mathrm{NO}} = 1076$ kJ mol^{-1}) [5], and thus there is a greater probability to find both molecular and dissociated NO on metallic surfaces. Molecular adsorption of NO has been reported for the noble metals and Pd and Pt, whereas dissociative adsorption dominates on the surfaces of Ni and of all other transition metals with an incompletely filled d-shell. For CO the dividing line between molecular and dissociative adsorption runs between the Fe- and Mn-groups. For NO both molecular and dissociative adsorption have been observed also on the late transition metals of the Ir- and Pt-groups: in some cases molecular adsorption has been reported at low temperatures, whereas at higher temperatures dissociation takes place [6]. The adsorption behaviour is also coverage-dependent: dissociation at low coverage can revert to molecular adsorption at higher coverage. The electronic spectrum of NO differs from that of CO by the occupation of the antibonding $2\pi^\star$ orbital by an unpaired electron. Hence it has been suggested that NO can either donate the $2\pi^\star$ electron to the substrate or accept electrons from the substrate to increase the filling of the $2\pi^\star$ level. This has led to the expectation a of wide variety of bonding situations, and of the possibility to adopt many different bonding geometries. However, a consensus on the favourite adsorption sites of NO on transition metal surfaces is still missing. Experimentally, a widely used approach to the determination of the adsorption geometry is to exploit the analogy between gas–surface interactions and organometallic coordination chemistry [7, 8]. The idea is to use vibrational frequencies from nitrosyl and carbonyl compounds measured by electron energy loss spectroscopy (EELS) or reflection-absorption infra-red spectroscopy (RAIRS) as the basis for the assignment of the NO and CO stretching frequencies to adsorption in a threefold hollow, a twofold bridge or in an on-top site. However, there is increasing evidence that this idea can be misleading [9–14].

An example for the failure of the assignment of the adsorption geometry based on vibrational data is NO on Ni(111). In agreement with an early EELS study [15], a RAIRS experiment by Erley [10] identified two vibrational bands which were assigned, on the basis of a comparison with the vibrational frequencies of nitrosyl compounds with known structures, to NO adsorbed in a bent twofold site and in a twofold bridge site. However, in an ESDIAD (electron stimulated desorption angular distribution) investigation Netzer and Maddey [9] found only upright NO species. A more recent SEXAFS (surface extended x-ray adsorption fine structure) study by Aminpirooz *et al* [11] led to contradictory results, demonstrating that NO adsorbs in a threefold hollow position and that the ratio of NO species adsorbed in fcc and hcp sites is 50:50. These conclusions were confirmed by photoelectron diffraction (PED) [12] and LEED (low-energy electron diffraction) [14] experiments. Theoretical studies of NO adsorption on Ni clusters [16] also predicted adsorption in a threefold site and calculated vibrational frequencies in good agreement with experiment.

Other NO adsorption systems that have been investigated using density-functional theory include Pt(111) [17], Rh(111) [18–20], Pd(111) [18, 19], Ir(111) [21], Pt(110) [22], Pt(100) [23, 24], Rh(100) and Pd(100) [19], and Rh, Pd and Pt(100) [25]. For all the

close-packed (111) surfaces the DFT calculations predict NO adsorption to occur in the threefold hollows, in disagreement with the original assignments of adsorption sites based on investigations of the vibrational spectra. Magnetic effects on the adsorption of paramagnetic NO on the nonmagnetic Cu(111) and Pt(111) surfaces were studied by Bogicevic and Hass [26]. The paramagnetic moment of the molecule is completely quenched upon adsorption, and no net magnetization of the adsorbate was found in several high- and low-coordinated adsorption geometries on either metal, in agreement with studies on NO/Ru(0001) by Hammer [27] and NO/Pt(111) by Ge and King [17]. However, Ge and King note a local spin-polarization in the Pt slab, resulting from the high magnetic susceptibility of Pt. But even in this case the influence of spin-polarization on the adsorption energy remains very modest: the adsorption energy of ∼1.75 eV for NO in a threefold hollow changes only by 10 meV if spin-polarization is considered. A comparative study of NO adsorption on non-magnetic Pd(100) and magnetic $Pd_3Mn(100)$ surfaces was reported by Delbecq and Sautet [28]. While on the pure Pd and on the segregated Pd_3Mn surface with a covering Pd-layer, an almost complete quenching of the paramagnetism of NO was reported, on stoichiometric Pd_3Mn surfaces NO shows a strong preference for adsorption at the strongly magnetic Mn surface atoms where it retains a substantial magnetization. For NO adsorbed on the ferromagnetic Ni(100) surface Hass *et al* [29] reported a nearly vanishing magnetic moment of NO and a strong local demagnetization of the Ni atoms directly linked with NO. Similar adsorbate-induced demagnetization was also reported for CO adsorption on Ni [30] and Fe [31] surfaces.

Recently Brown *et al* [2] have presented a critical review of the chemisorption of NO on metal surfaces, concentrating in particular on the site assignment for NO adsorption based on measured vibrational frequencies. In the past the following NO stretching frequencies from inorganic metal–nitrosyl complexes have been used as the basis for adsorption-site assignments [2]: threefold nitrosyls 1320–1545 cm^{-1}, twofold nitrosyls 1480–1545 cm^{-1}, linear on-top 1650–2000 cm^{-1}, and bent on-top 1525–1700 cm^{-1}. Evidently there is a lot of overlap between the frequency intervals attributed to the different adsorption species, and in addition widely varying frequencies have been reported for similar adsorption systems (to be discussed in more detail below). On the basis of a critical confrontation of vibrational studies using EELS and RAIRS, structural investigations based on SEXAFS, LEED, ESDIAD and PED, and of theoretical studies based on DFT, a new basis for the vibrational site assignment was elaborated. Following the study of Perez-Jigato and co-workers [32], the proposed N–O stretching frequency bands and the corresponding sites are the following: 1450–1645 cm^{-1} for threefold coordinated NO; 1640–1710 cm^{-1} for bridge-adsorbed NO, and 1700–1850 cm^{-1} for on-top-adsorbed NO. However, it was also pointed out that the frequency ranges characteristic for the different sites depend on the surface on which adsorption occurs. Hence even the redefined frequency ranges must be used with some caution for site assignment.

Under these circumstances systematic theoretical studies of the trends in the adsorption energies, site preference and adsorption geometry, and vibrational properties of NO adsorbed on transition metal (TM) surfaces, replacing earlier studies performed with different techniques and different computational set-ups are highly desirable. So far such a systematic study has been performed only for small TM_4 clusters with a tetrahedral geometry [33], but evidently the adsorption properties on these clusters will differ quite strongly from those on flat, close-packed surfaces. In this paper we present an extensive density functional study of the molecular adsorption of NO on the close-packed surfaces (i.e. (111) for fcc, and (0001) for hcp structures) of Co, Ni, Cu, Ru, Rh, Pd, Ag, Ir, Pt and Au. In a recent paper [3] we have investigated CO adsorption, especially the trend in the structural, vibrational and electronic properties and the correlation between them for the same set of metals, with the site preference as a key issue. The structure of the present paper is similar. Section 2 reviews very briefly the underlying

methodology and presents the set-up of our calculations. Section 3 presents our results for the geometric structure, vibrational and electronic properties of the NO/metal adsorption complexes. Our results are discussed in the light of available experimental and theoretical literature. Correlations between the investigated properties are analysed. A forthcoming study will cover the dissociative adsorption of NO on these surfaces.

2. Methodology and computational set-up

The calculations in this work are performed using the Vienna *ab initio* simulation package VASP [34, 35] which is a DFT code, working in a plane-wave basis set. The electron–ion interaction is described using the projector-augmented-wave (PAW) method [35, 36] with plane waves up to an energy of $E_{\mathrm{cut}} = 450$ eV (for convergence checks some calculations with harder pseudopotentials for N and O requiring an energy cut-off of 700 eV have been performed).

For exchange and correlation the functional proposed by Perdew and Zunger [37] is used, adding (semi-local) generalized gradient corrections (GGA) according to Perdew *et al* (PW91) [38]. It has been suggested that the gradient-corrected functional of Perdew, Burke and Erzernhof, as revised by Hammer *et al* [39] (RPBE), leads to a better predictions of the adsorption properties. In [3] we have carefully compared the performance of both functionals in describing CO adsorption. The conclusion was that although the RPBE functional leads to lower adsorption energies in better agreement with experiment, it does not solve the problem of the prediction of wrong adsorption sites on a number of surfaces (Pt, Cu, Rh): all current GGA functionals tend to overestimate the adsorption energy for the sites with high metal coordination compared to sites with low metal coordination. For CO it has been shown that this is directly related to the underestimation of the HOMO–LUMO gap facilitating back-donation into the $2\pi^\star$ orbital. The problem of the prediction of the correct adsorption site for CO can be solved only by post-DFT techniques shifting the LUMO to higher energies [40–42]. For NO with a partially filled $2\pi^\star$ state pinned at the Fermi level we expect this problem to be of minor importance. The RPBE and PW91 functionals lead to very similar results for the adsorption geometry and the vibrational properties. For the description of the pure metallic surfaces, PW91 is slightly superior to RPBE (see [3] for details). In the present work we examine the change of the adsorption energies on replacing the PW91 by the RPBE functional, but not the change in the other adsorption properties. Spin-polarized calculations have been performed for NO adsorbed on the surfaces of the ferromagnetic metals Co and Ni. In addition, spin-polarized calculations have been performed for NO on Ag(111) and Pt(111) to check the interplay between the paramagnetic moment of the adsorbate and the polarizability of the noble or transition metal substrate. Anticipating the results, we note that for the non-magnetic substrates, spin-polarization effects were found to be very small, in agreement with previous studies. Hence the results of non-spin-polarized calculations are presented.

The adsorption of NO on the close-packed surfaces (i.e. (111) for fcc and (0001) for hcp) of Co (hcp), Ni, Cu (both fcc) in the 3d series, Ru (hcp), Rh, Pd, Ag (all fcc) in the 4d series, and Ir, Pt and Au (all fcc) in the 5d series has been studied. The metallic surface is modelled by a slab consisting of four layers of metal separated by a vacuum layer of approximately the same thickness, as shown in figure 1. The two uppermost substrate layers and the NO molecule are allowed to relax. It is well known that to achieve convergence with respect to all details of the surface electronic structure, considerably thicker slabs are required. However, many *ab initio* studies of atomic and molecular adsorption have also demonstrated that properties depending only on the total energy of the adsorbate–substrate complex are much less sensitive to the number of monolayers in the slab used to model the surface. Our choice of four-layer

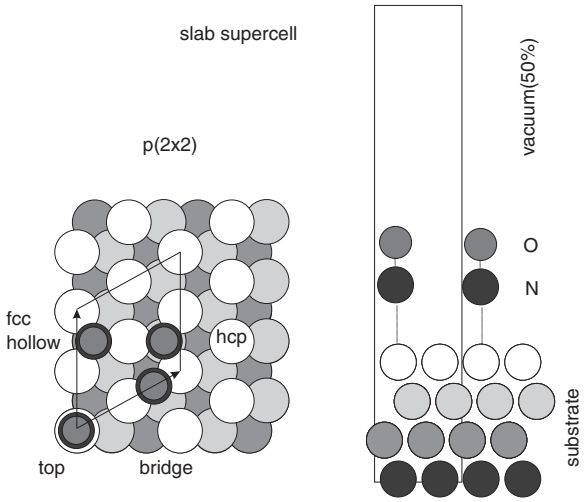

Figure 1. Slab model for the close-packed surfaces. The p(2 × 2) surface cell with all high symmetry sites for the adsorption of an NO molecule is shown on the left, and a side view of the system on the right.

slabs represents a compromise between accuracy (absolute values of adsorption energies are converged to about 0.03 eV/molecule, much better convergence at the meV level is achieved for the differences between adsorption geometries) and the necessity to keep the computational effort within bounds, as required for such a comprehensive analysis of many different surfaces.

We have considered four on-surface sites: top, bridge, and fcc and hcp hollow sites in p(2 × 2) and c(2 × 4) arrangements, corresponding to a coverage of $\Theta = 0.25$ ML. However, we have to stick to the p(2 × 2) overlayer for which the adsorbate interactions are smaller. Γ-point centred grids of (4 × 4 × 1) and (8 × 8 × 1) k-points are used for most Brillouin zone integrations; (10 × 10 × 1) grids have been used to converge the smallest energy differences. Careful convergence tests for the slab thickness and k-space grids have been performed in our recent study of CO on close-packed metal surfaces [3].

A conjugate-gradient algorithm is used to relax the ions into their ground-state locations [43]. Equilibrium is reached if the force on the atoms is less than 0.04 eV Å^{-1} in each of the Cartesian directions. Vibrational frequencies for the metal–NO ($\nu_{\mathrm{M-NO}}$) and intramolecular N–O stretching modes ($\nu_{\mathrm{N-O}}$) were computed by applying a finite-differences method where the substrate is frozen and NO is allowed to vibrate in any direction. The change of the dipole moment strongly influences the intensity of the vibrational frequencies and is the sign of possible tilting of the NO molecule. The choice of a 'low' coverage phase (0.25 ML) is also motivated by the fact that the dynamical dipole moment is significantly altered at the highest coverage with a highly close-packed structure [44].

The electrostatic interaction between the adsorbates depends on the actual effective charge of the species and the distance between the dipoles, which is around 4 Å. The repulsive lateral interactions between the adsorbates influence the heat of adsorption of the molecules. However, the radius of the electronic effects mediated by the surface is believed not to exceed ∼5 Å. With our set-up (p(2 × 2)) the minimal distance between neighbouring adsorbates varies between 5.0 Å (Co) and 5.9 Å (Au) and adsorbate–adsorbate interactions are expected to be weak. LEED studies confirmed relatively weak long-range interactions of the NO molecules on the Co(10$\bar{1}$0) surface [44].

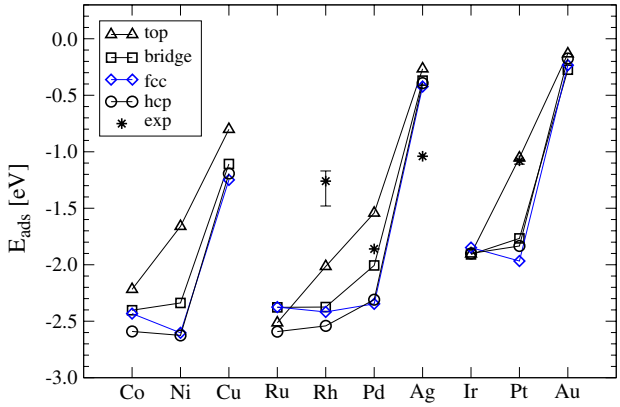

Figure 2. Calculated NO adsorption energies on transition metal and noble metal surfaces. Experimental heats of desorption are represented by asterisks (for references see text and table 1), calculated adsorption energies for top sites are presented by triangles, for bridge sites by squares, for fcc hollows by diamonds, and for hcp hollows by circles. The PW91 exchange–correlation functional and a plane-wave cut-off $E_{\mathrm{cut}} = 450$ eV were used.

The theoretical results for the properties of the pure (111) surfaces (lattice constant, work function, electronic structure) have been presented in [3]. The experimental equilibrium bond length and stretching frequency of the free NO molecule are 1.148 Å and $\nu_{\mathrm{N-O}} = 1903\ \mathrm{cm}^{-1}$ [45]. The corresponding calculated values are 1.168 Å and 1917 cm^{-1} (harmonic stretching frequencies). The calculated molecular binding energy is $E_{\mathrm{NO}}^{\mathrm{GGA}} = 7.46$ eV and the experimental value of $E_{\mathrm{NO}}^{\mathrm{exp}}$ is equal to 6.63 eV [46]. The difference between theory and experiments is 12.5%, which is greater than for the CO molecule (2.7%) [3].

3. NO adsorption

3.1. Site preference and adsorption energies

What is the site preference for NO adsorption? The experimental and the corresponding theoretical adsorption energies for all four high-symmetry sites are collected in figure 2. The calculated adsorption energies show that with the sole exception of NO/Ir(111), NO in a hollow site has the largest adsorption energy on all surfaces, or the adsorption energy for the hollow is nearly degenerate with that for the bridge, or even with the bridge and the top site. A clear preference for adsorption in a threefold site is found for Co, Ni, Ru, Rh, Pd, and Pt. Preference changes from the hcp hollow site on Co, Ni, Ru, and Rh surfaces to the fcc hollow site on Cu, Pd, and Pt. However, the difference in adsorption energies in the fcc and hcp hollow sites is only very small for Ni (∼30 meV) and for Pd (∼40 meV). Interestingly, all three high-symmetry adsorption sites are almost degenerate on Ir(111), where the top site is preferred by ∼30 meV over the bridge site and by ∼40 meV over the hollow sites. However, a very dense k-point mesh ($10 \times 10 \times 1$) is required to achieve convergence of the differences in the adsorption energy at this level. Vibrational spectroscopy [47] distinguishes stretching frequencies at 1860, 1550, and 1440 cm^{-1}, with the largest intensity on the high-frequency mode. This is compatible with a disordered distribution of the adsorbate over all three types of site expected on the basis of our results. A quasi-degeneracy of top, bridge and hollow sites on Ir(111) has also been reported by Krekelberg *et al* [21]. A further interesting case is NO/Ru(001) where we find the largest difference between the adsorption energies in the fcc

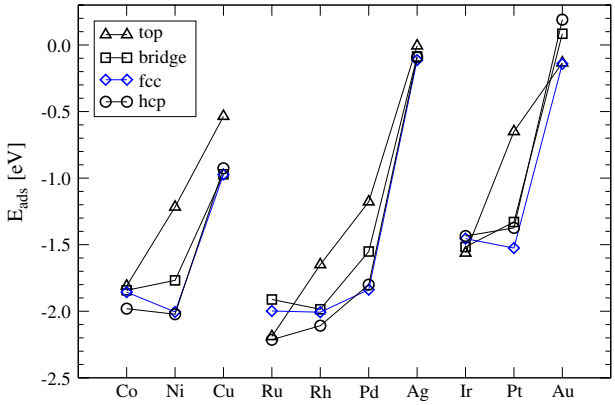

Figure 3. Calculated NO adsorption energies on transition metal and noble metal surfaces. Top sites are presented by triangles, bridge sites by squares, for fcc hollows by diamonds, and for hcp hollows by circles. The RPBE exchange–correlation functional and a plane-wave cut-off $E_{\mathrm{cut}} = 450$ eV were used.

and hcp hollow sites, and a relatively strong on-top adsorption with an energy intermediate between that calculated for the two types of hollow.

The predicted site preference does not change if the PW91 exchange–correlation functional is replaced by the RPBE functional, see figure 3. Although the absolute values of the adsorption energies are reduced by about 0.4 eV/molecule the energetic ordering remains the same. In a few cases we note minor changes in the structural energy differences, but the near degeneracy of all adsorption sites on Ir(111) and of the fcc and top sites on Ru(0001) are also found with the RPBE functional. A qualitative change occurs only for adsorption on the surfaces of the heavy noble metals Ag and Au: on Ag, NO is predicted to be almost unbound, irrespective of the adsorption site, while on Au a weak adsorption is found on the top and fcc sites, while NO is unbound on the bridge and hcp sites. Hence, while for the transition metals the RPBE functional leads to a better agreement of the calculated adsorption energies with experiment, the PW91 results are more realistic for the noble metals. For a detailed confrontation of theory and experiment, see the following subsection.

Altogether, the site preference predicted by our calculations is in good agreement with the revised site assignments reviewed by Brown and King [2]. The small differences in the adsorption energies for the threefold and twofold sites suggest that NO on these surfaces is a highly mobile species, with an activation energy for diffusion (as measured by the difference in the adsorption energies in the hollow and in the bridge sites) not exceeding 0.3 eV. The exception is the Ru(0001) surface where diffusion between the hexagonal hollows across the top site has a lower activation energy. For NO/Ir(111) a first look at the adsorption energies calculated for the high-symmetry sites suggests an energy barrier for NO diffusion along a top-bridge-top path of only 30 meV (PW91) and 100 meV (RPBE) respectively. A more detailed exploration of the potential energy surface (PES) for NO diffusion on Ir(111) leads to a quite surprising result (see figure 4): the absolute PES minimum at the top site is separated from the local minima at the hollows by substantial barriers of about 0.3–0.4 eV, and the barrier for diffusion from top to bridge is still about 0.28 eV. This demonstrates that diffusion barriers should not be estimated from the adsorption energies in high-symmetry sites alone. The consequences of the form of the PES on the adsorption dynamics of NO on Ir(111) will be discussed in more detail below (see section 3.1.2). For Pd(111) and Pt(111) we find the

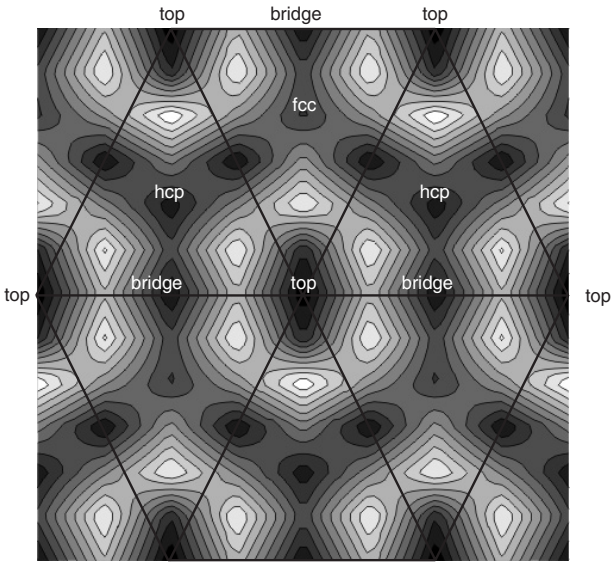

Figure 4. Contour plot of the potential energy surface for adsorption of NO on Ir(111), as calculated using the PW91 functional. Darker regions indicate a higher adsorption energy for the NO molecule. The change of the adsorption energy between two neighbouring contours is 40 meV. Note the existence of barriers surrounding the absolute minimum at the top site; see the text.

bridge position to be unstable; it corresponds only to a saddle point on the potential-energy surface, with an imaginary eigenfrequency for one of the frustrated translation modes.

3.1.1. Comparison with experiment. For the absolute values of the adsorption energies the difference between theory and experiment is large; see table 1. However, in contrast to CO, only a few experimental results from thermal desorption spectroscopy (TDS) are available for NO. For Rh and Pt, our adsorption energies calculated using PW91 are about 1 eV larger than experiment. This discrepancy is reduced to about 0.5 eV if the RPBE functional is used. A similar difference between the adsorption energies calculated using the two functionals has also been reported by Krekelberg *et al* [21] for Ir(111), by Mavrikakis *et al* [20] for Rh(111), and by Hansen *et al* [48] for Pd(111). Surprisingly, for Pd, the difference between experiment and PW91 is only 0.5 eV, and the RPBE adsorption energy even matches the experimental result perfectly. It is also quite surprising that, for NO/Ag(111), the adsorption energy reported from the TDS experiment is twice as large as our PW91 prediction.

However, it must be emphasized that the results of a comparison of the calculated adsorption energies with those derived from the measured temperature-programmed desorption (TPD) spectra must be interpreted with some caution: TPD experiments deliver *differential* desorption energies, while the calculations yield integral adsorption energies. The calculations are for $T = 0$ K; the experiments refer to finite temperatures. It is also legitimate to question the accuracy of the experimental results. More reliable results than from TPD spectra can be obtained via microcalorimetric measurements: for NO/Pt(111) Wartnaby *et al* [49] reported an adsorption energy of 1.66 eV for coverages up to 0.25 ML, evidently in much closer agreement with the results of the DFT calculations.

The confrontation of experimental results for different metals also leads to evident contradictions to the trends expected on the basis of sound physical arguments. From the

Table 1. Experimental and calculated adsorption energies of NO on transition metal and noble metal surfaces. Experimental results are from temperature-programmed desorption (TPD), thermal desorption spectroscopy (TDS) and microcalorimetric (MC) measurements.

Surface	E_{ads} (exp.)	Method	Reference	E_{ads}^{PW91} (calc.)	E_{ads}^{RPBE} (calc.)
Rh(111)	−1.26	TPD	[50]	−2.54	−2.11
	−1.48		[51]	—	—
	−1.17	TPD	[52]	—	—
Pd(111)	−1.86	TPD	[53]	−2.35	−1.84
Ag(111)	−1.04	TDS	[54]	−0.43	−0.11
Pt(111)	−1.08	TPD	[55]	−1.97	−1.53
	−1.17		[56]	—	—
	−1.11		[57]	—	—
	−1.66	MC	[49]	—	—
Pt polycrystal	−0.36	TPD	[58]	—	—

experimental results on CO adsorption, and from our trends for the variation of the adsorption energy with band-filling, we would expect only a small variation of the adsorption energy from Rh to Pd, a modest decrease as the centre of the d-band moves away from the Fermi edge. The strong increase suggested by the available experimental data (see table 1) is in evident contradiction to the expected trend and to the small decrease found in the calculated adsorption energies. Also an adsorption energy of 1 eV for NO/Ag(111), i.e. almost as large as for NO/Pt(111), appears to be unrealistically large for a noble metal surface. Further experimental studies are urgently needed to assess the quality of the DFT predictions for the adsorption energy of NO on transition metal surfaces.

3.1.2. A case study for NO on Ir(111): coexisting adsorption geometries and unconventional diffusion scenario. The near degeneracy of the adsorption energies and the observation of three distinct NO-stretching modes in EELS experiments [47] makes NO on Ir(111) a particularly interesting system for study. Davis *et al* [47] have investigated the kinetics and dynamics of the initial adsorption of NO on Ir(111) using supersonic molecular beam techniques and EELS and concluded that separate mechanisms govern adsorption at low and high kinetic energy of the incident molecules. Adsorption at low kinetic energy, low temperature and low coverage produces an adsorbate characterized by a single loss feature at 1860 cm^{-1} in the EEL spectra. Increasing coverage produces an additional loss feature at 1550 cm^{-1} and after a further increase also at 1440 cm^{-1}. For high kinetic energies the additional modes at lower frequencies appear already at lower coverages and with higher intensity. These results have been interpreted in terms of coexisting physisorbed and chemisorbed species: at low kinetic energy and low temperature, NO is first physisorbed. With increasing temperature and coverage, this physisorbed species undergoes a transformation to a chemisorbed state. At high kinetic energy, NO adsorption occurs directly into the chemisorbed state, albeit with a finite probability of trapping in the physisorbed state.

Our detailed map of the PES of NO on Ir(111) (see figure 4) suggests a different interpretation. The absolute minimum of the PES is located at the top site and surrounded in all directions by barriers of 0.2–0.3 eV. Molecules impinging on the surface with low kinetic energies will be efficiently steered into this potential well [59, 60]. The steering is the more efficient as the molecule binds to the top site mainly through the d_{z^2} states which have the largest extension perpendicular to the surface. With increasing surface coverage, certain top

sites are blocked and molecules are also trapped in neighbouring potential wells: bridge sites, and also hcp hollows. At increasing temperature, activated hopping across the potential barriers becomes possible, and in addition to the top sites, bridge and hollow sites are populated in thermal equilibrium, favoured by the small structural differences in the adsorption energies. At high kinetic energies, steering is less efficient, and initial adsorption occurs also in the energetically only slightly less favourable hollow and bridge sites.

The calculated harmonic NO-stretching frequencies of 1898, 1646, and 1503 cm^{-1} for top-, bridge-, and hollow-adsorbed NO are in reasonable agreement with the experimentally observed loss features at 1860, 1550, and 1440 cm^{-1} (anharmonic corrections will account for most of the difference). However, it is certainly a bit surprising that the top-adsorbed species which undergoes only the smallest red-shift of the NO-stretching frequency is also the most strongly bound. Evidently this excludes an assignment of this vibrational mode to a physisorbed NO molecule.

The small site-dependent variation of the adsorption energies and the form of the PES also leads to a quite unusual scenario for NO diffusion on the Ir(111) surface. An activation energy of 0.28 eV is necessary for a hopping of the molecule from a top to a bridge site. Hopping from top to hollow requires an even higher activation energy of 0.36 eV, but given the anisotropic form of the potential well surrounding the top site (see figure 4), part of the difference is probably made up by a larger prefactor resulting from a lower frequency for the frustrated translation mode. The activation energies for these processes are of the same order or even slightly higher than for NO diffusion on other surfaces. For the migration from bridge to hollow and vice versa, however, the activation energies are only 40–60 meV (with saddle points located at off-symmetry positions) so that a molecule can diffuse very rapidly along the narrow channels connecting these sites.

3.1.3. Comparison with earlier theoretical calculations. For Ru, Rh, Ir, Pd, and Pt, earlier theoretical studies of NO adsorption are available in the literature. In table 2 the adsorption energies calculated using different approaches are compiled. Before going into a discussion of the evident differences in the results, a few brief comments on the methods are necessary. The VASP[1], DACAPO[2], CASTEP[3], FINGER[4], and STATE[5] codes use a plane-wave basis set. However, whereas VASP is available in an all-electron version based on the projector-augmented wave method (PAW: this is the approach adopted in the present work) and in a pseudopotential version with ultrasoft pseudopotentials (US-PPs), the other four codes use only pseudopotentials. The calculations using DACAPO are all based on ultrasoft pseudopotentials for both the substrate and the atoms forming the molecule. The calculation for Pd using the FINGER code uses US-PPs only for the N and O atoms, and norm-conserving (NC) PPs for Pd. The calculation for Pt based on CASTEP uses NC-PPs for all atoms. The choice of the potential is decisive for accuracy and basis-set convergence. A cut-off energy of 450 eV was used in the present work, test calculations using a cut-off of 700 eV confirm that the adsorption energies change by at most 0.02–0.05 eV if the cut-off is so strongly increased. Most other VASP calculations use a slightly lower cut-off of 400 eV; in the DACAPO calculations a cut-off of 340 eV is standard. The lower cut-off leads to a slightly reduced accuracy. However, a cut-off of 340 eV for US-PPs is still much better than a cut-off of only 500 eV for calculations

[1] The Vienna *ab initio* simulation package was developed by Kresse *et al* [34, 35, 98].
[2] The DACAPO package was developed at the Technical University of Denmark by Hammer *et al* [99].
[3] The CASTEP package was developed at the University of Cambridge by Payne *et al* [100].
[4] The FINGER code has been developed at Helsinki University of Technology. It is based largely on methods described in the paper by Laasonen *et al* [101].
[5] The STATE package was developed by Morikawa *et al* [102].

Table 2. Adsorption energies (in eV/molecule) for NO on close-packed transition metal and noble metal surfaces, as calculated using different techniques. See the text.

Surface	Reference	Method	Exch.–correl. functional	Coverage (ML)	Top	Bridge	fcc	hcp
Ru	This work	VASP/PAW	PW91	0.25	−2.51	−2.38	−2.38	**−2.59**
			PW91	0.0625	−2.57	—	—	—
			RPBE	0.25	−2.19	−1.91	−2.00	**−2.21**
	[61]	DACAPO/USPP	PW91	0.125	−2.14	−2.40	−2.49	**−2.73**
	[62]	ADF cluster	B88 + P86	—	−1.63	—	−2.05	—
Rh	This work	VASP/PAW	PW91	0.25	−2.01	−2.37	−2.42	**−2.54**
			RPBE	0.25	−1.65	−1.99	−2.01	**−2.11**
	[63]	VASP/USPP	PW91	0.25	−1.91	−2.26	−2.38	**−2.47**
	[18]	VASP/USPP	PW91	0.33	−1.90	−2.27	−2.45	**−2.50**
	[20]	DACAPO/USPP	PW91	0.25	−1.98	−2.25	−2.26	**−2.39**
			RPBE		−1.53	−1.73	−1.72	**−1.83**
	[64]	ADF	B88 + P86	0.33	−1.38	−1.97	−2.14	**−2.18**
Pd	This work	VASP/PAW	PW91	0.25	−1.54[a]	−2.03	**−2.35**	−2.31
			RPBE	0.25	−1.18[a]	−1.55	**−1.84**	−1.80
	[18]	VASP/USPP	PW91	0.33	−1.09	−1.96	**−2.29**	−2.26
	[65]	FINGER/NCPP	PBE	0.25	−1.10	−1.93	**−2.26**	−2.24
	[48]	DACAPO/USPP	PW91	0.16	−1.05	−1.92	**−2.29**	—
			RPBE	0.16	−0.66	−1.45	**−1.80**	—
			PW91	0.33	—	—	**−2.22**	−2.21
			RPBE	0.33	—	—	**−1.72**	−1.71
	[64]	ADF	B88 + P86	0.33	−1.17	−1.69	**−2.00**	−1.96
	[62]	ADF cluster	B88 + P86	—	−1.13	—	−2.27	—
	[32]	CADPAC	B3P86	—	−0.42	**−1.92**	−0.71	—
Ir	This work	VASP/PAW	PW91	0.25	**−1.91**	−1.88	−1.81	−1.87
			RPBE	0.25	**−1.56**	−1.52	−1.45	−1.43
	[21]	DACAPO/USPP	PW91	0.25	**−1.81**	−1.80	−1.68	−1.72
			RPBE		**−1.38**	−1.30	−1.14	−1.14
	[62]	ADF cluster	B88 + P86	—	−1.23	—	−1.98	—
Pt	This work	VASP/PAW	PW91	0.25	−1.56[a]	−1.77	**−1.97**	−1.83
			RPBE	0.25	−0.65[a]	−1.35[b]	**−1.53**	−1.37
	[26]	VASP/USPP	PW91	0.16	−1.60	−1.79	**−2.02**	−1.92
	[17]	CASTEP/NCPP	PW91	0.25	−0.64	−1.43	**−1.75**	−1.655
	[66]	STATE/USPP	PBE	0.25	−1.61	−1.92	**−2.09**	−1.92
	[62]	ADF cluster	B88 + P86	—	−0.49	—	−1.70	—

[a] Tilted adsorption geometry; see the text.
[b] In RPBE calculations the bridge adsorption site is found to be unstable; the molecule moves to the fcc hollow. The adsorption energy quoted here refers to a molecule with the N atoms fixed on the bridge site and a tilt of the molecular axis. See the text.

with an NC-PP for transition metals. Basis-set convergence is more problematic to judge for calculations using localized basis sets such as ADF[6]. ADF exists in a periodic and in a cluster version; it is well known that convergence with increasing cluster size towards the periodic

[6] The ADF-Band Package has been developed at the Laboratory of Theoretical Chemistry, Free University of Amsterdam; see te Velde and Baerends [103].

results is sometimes quite slow [40]. A further factor affecting the accuracy of the calculations is the choice of the k-point set for Brillouin zone integrations: not all published calculations are necessarily fully converged. For the sake of completeness, we have also included in the comparison a calculation using CADPAC[7] which allows one to examine the influence of hybrid functionals mixing DFT and Hartree–Fock exchange.

The choice of the exchange–correlation functional has a larger influence on the calculated adsorption energies than that of the basis sets or of the potential. The largest database is available for NO/Pd(111). All calculations using PAWs or PPs and the PW91 or the (R)PBE functionals predict adsorption in the fcc hollow, with adsorption energies ranging between 2.26 and 2.35 eV at a coverage of 0.25 ML (taking the average between the lower and higher coverages reported in the DACAPO calculations; these results also demonstrate a quite modest coverage dependence of the adsorption energies). The energy differences for adsorption in the hcp hollow or in the bridge sites also agree within ± 0.01 eV; larger discrepancies exist for on-top adsorption. Calculations using the RPBE functional lead to a reduction of the adsorption energy by 0.5 eV, without affecting the structural energy differences. However, one has to note that most RPBE calculations are non-selfconsistent, i.e. they have been performed using the geometries and charge-densities from the PW91 optimizations. The reason is that RPBE predictions for the properties of the clean substrate are always less accurate than the PW91 results (see [3] for details). The periodic ADF calculations using a different DFT functional predict the same site preference and very similar structural energy differences between bridge and hollow, but absolute values of the adsorption energy intermediate between the PW91 and RPBE results. ADF cluster calculations on 13-atom clusters produce a stronger preference for adsorption in a hollow than periodic calculations. This is in agreement with the findings of Kresse *et al* [40, 67] for CO on Pt(111), who reported that the preference for highly coordinated adsorption sites decreases with increasing cluster size. A CADPAC cluster-calculation using a hybrid-functional mixing DFT and Hartree–Fock exchange leads to completely different results, with a very strong (and unrealistic) preference for bridge-site adsorption. Hybrid functionals are an interesting alternative to DFT functionals because of their tendency to produce larger HOMO–LUMO gaps and lower (and hence more realistic) binding energies. However, most applications of hybrid functionals are restricted to molecules and insulating solids. For metals the mixing of DFT and exact (i.e. Hartree–Fock) exchange might be problematic, given the singularity of the exchange operator at the Fermi level. As current implementations of hybrid functionals in cluster codes do not allow one to reach convergence with respect to cluster size, and implementations of hybrid functionals in periodic codes are still in the testing stage, it remains to be seen whether they will represent a viable alternative for improving molecular adsorption energies on metallic surfaces.

A similar conclusion as for NO/Pd(111) also derives from the data for NO on Rh(111) and Ru(0001), but in this case we note a somewhat larger difference between the VASP and DACAPO calculations. Results for the most weakly bound adsorption configuration (the top site) are found to be most sensitive to parameters determining basis-set and k-point convergence. In addition the selfconsistent RPBE calculation in the present work leads to a more modest reduction of the adsorption energy compared to the PW91 result than the non-selfconsistent calculations based on DACAPO. For NO/Ir(111) both VASP and DACAPO calculations agree on the quasi-degeneracy of top and bridge adsorption, with slightly larger adsorption energies resulting from the VASP/PAW calculations. ADF cluster calculations predict again a very strong preference for adsorption in a hollow. For NO/Pt(111), results for

[7] The Cambridge Analytical Derivative Package developed by R D Amos uses numerical quadrature and requires no specification of a basis set.

four different sets of plane-wave calculations and one cluster calculation are available. The PW calculations agree on the preference for adsorption in the fcc hollow and on the energy difference between the fcc and hcp hollows. The scatter for the other energy differences are substantially larger. The calculations using CASTEP and NC pseudopotentials also predict much lower values for the adsorption energies, although the same PW91 functional has been used. Part of the difference has to be attributed to constraints imposed during the relaxation of the adsorbate/substrate system. While in the present work, the two top layers of the substrate are allowed to relax, the CASTEP calculations of Ge and King [17] admit a rigid substrate. Only for adsorption in the fcc hollow has relaxation of one top layer been considered. This leads to an increase of the adsorption energy from 1.75 to 1.89 eV, making up for two thirds of the difference compared to the present work. The CASTEP and cluster calculations for NO/Pt(111) also predict an unrealistically large difference in adsorption energy for hollow and top sites, resulting both from finite-size effects and the neglect of relaxation.

Altogether this analysis demonstrates that although state-of-the-art calculations agree tolerably well in predicting the adsorption properties of selected systems, the dependence on the computational set-up (cut-off energies or basis set, k-point mesh for Brillouin zone integration, etc) is strong enough to obscure any systematic trends determined by the substrate. To elucidate these trends, a unified approach is required.

3.2. Influence of spin polarization

It is well established, both experimentally [68] and theoretically (see [3]), that the adsorption of CO on Ni(100) strongly reduces the magnetic moments of the Ni atoms to which the molecule bonds. Similar effects have been reported for CO adsorbed on α- and γ-Fe [69, 70]. For NO adsorption the situation is even more complex because of the paramagnetic moment of the molecule in the gas phase. Hass *et al* [29] have used DFT in the local-density approximation to investigate NO adsorption on the (100) surfaces of Ni, Rh, Pd, and Pt. For bridge-adsorbed NO on Ni(100), a complete quenching of the magnetic moments to which the NO bonds, as well as vanishing magnetic moments of the N and O atoms, is reported. For on-top adsorption the Ni surface atom directly bonded to the aligned NO molecule conserves a magnetic moment. The results for the non-magnetic metals cannot be considered as representative, because the calculations for three-layer slabs predict magnetic ordering of the Pd and Pt surfaces [29] which is not confirmed by more recent studies. Similarly, for NO/Pt(111), Ge and King [17] reported a complete loss of the magnetic moment of the adsorbed molecule, accompanied by a local induced magnetic polarization of the substrate. The induced magnetization is strongly size-dependent: the local polarization is found for a six-layer slab, but disappears if the slab thickness is reduced to four monolayers. However, a possible local polarization of the substrate has only an almost negligible effect on the adsorption energy. For NO on Cu(111) and Pt(111), Bogicevic and Hass [26], and for NO/Ru(0001) Hammer [27], reported a complete quenching of the paramagnetic moment of the molecule, independent of the adsorption geometry, and only a negligible induced polarization of the substrate.

We have recalculated adsorption properties of NO on the ferromagnetic metals Co and Ni, on the noble metals Cu and Ag, and on Pt and Rh as an example of a non-magnetic heavy transition metal using a spin-polarized approach. Local magnetic moments have been calculated by projecting the plane-wave components of the spin-polarized eigenstates onto spherical waves within atomic spheres. It is evident that this decomposition is only an approximate one and can at best produce an estimate of the local magnetic moments. This is the reason that the atomic moments of N and O do not add to exactly one Bohr magneton for the NO molecule.

Table 3. The total magnetic moments of N and O atoms of NO molecule adsorbed on (111) surfaces. The magnetic moments of the interacting surface atoms are presented as surface. The magnetic moments are given in μ_B.

Surface	Atom	Clean	Top	Bridge	fcc	hcp
Co(111)	Co	1.78	0.63	1.11	1.28	1.26
	N	0.46	−0.07	−0.09	−0.07	−0.09
	O	0.25	−0.09	−0.15	−0.13	−0.14
Ni(111)	Ni	0.75	0.14	0.19	0.25	0.23
	N	0.46	−0.003	−0.02	−0.03	−0.02
	O	0.25	−0.02	−0.05	−0.06	−0.05
Ag(111)	Ag	0.0	0.02	—	0.02	—
	N	0.46	0.35	—	0.22	—
	O	0.25	0.29	—	0.25	—

The magnetic moments of Co and Ni atoms in the first layers of the clean Co(0001) and Ni(111) surfaces are slightly enhanced above the respective bulk values of 1.62 and 0.66 μ_B to 1.78 and 0.7 μ_B, respectively for Co and Ni. The adsorption of NO decreases the magnetic moment of the substrate atoms bonding with NO. The magnetic moment of Co atoms decreases to 0.6 μ_B for NO adsorbed in top sites, to 1.1 μ_B for bridge, and to 1.3 μ_B for NO in hollow sites (see table 3). The NO molecule conserves a small magnetic moment of the order of 0.2 μ_B; the orientation of the molecular moment is antiparallel to the substrate. For NO on Ni(111), the magnetic moment is quenched due to NO adsorption to 0.14 μ_B for Ni atoms bonding with NO in top sites, 0.2 μ_B for bridge, 0.25 μ_B for fcc hollow and 0.23 μ_B for hcp hollow sites. In this case both the N and O atoms are essentially completely demagnetized. The demagnetization of the substrate atoms is caused by a shift of the d-band of the bonding atom to higher binding energies, the demagnetization of the adsorbate by the donation from the 5σ and the back-donation to the $2\pi^\star$ orbital.

An NO molecule adsorbed on Cu(111) surface loses its magnetic moment completely, and the adsorption energy as well as structure remain almost unchanged ($\Delta E_{ads} \leqslant 5$ meV). In contrast, NO remains paramagnetic on Ag(111). For on-top adsorption, the magnetic moment of 0.35 μ_B for N atoms and 0.29 μ_B for O atoms adsorbed in the top site on Ag(111) increases the adsorption energy by 60 meV. For NO in an fcc hollow, the non-vanishing magnetic moment 0.22 μ_B for N atoms and 0.25 μ_B for O atoms adsorbed in the fcc hollow leads to an increase of adsorption energy by 20 meV. In both cases the changes of the adsorption energies are modest, and the adsorption induces only a negligibly weak magnetic polarization of the substrate atoms. The difference in the magnetic properties of the adsorbed NO atom reflects the much stronger binding to the Cu(111) than to the Ag(111) surface (cf figure 2), associated with a much stronger backdonation filling the $2\pi^\star$ orbital. For NO adsorbed on Pt(111) or Rh(111) no spin-polarization effects have been detected: the adsorbed molecule loses its magnetic moment, and no induced polarization of the substrate has been found. The contrast between NO on Cu(111) and Ag(111) is quite interesting; this is another example for the well-known fact that the chemical reactivity of Cu is much closer to that of the transition metals than for the heavier noble metals.

3.3. Structural properties

Bonding of both NO and CO to metallic substrates is determined by the balance between electron donation from the occupied 5σ states of the molecule to the substrate and backdonation

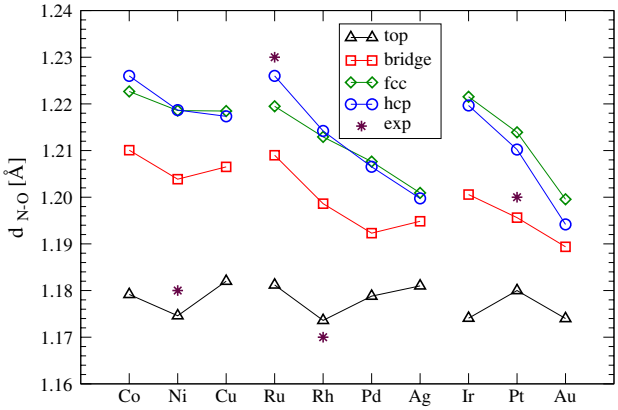

Figure 5. Trends in the calculated N–O bond lengths for adsorption in top, bridge, fcc and hcp hollow sites on transition metal and noble metal surfaces. Solid lines are a guide to the eye only. For experimental values, see table 4 and text.

from the metal to the antibonding $2\pi^\star$ orbital of the adsorbate. Whereas in a linear adsorption geometry 5σ donation is dominant, adsorption in bridge or hollow sites favours $2\pi^\star$ backdonation, leading to a weakening of the intramolecular bond. Hence increasing coordination of the adsorbate is expected to lead to an increase of the N–O bond length. On the other hand, according to steric and bond-order conservation arguments, the metal–nitrogen distance should increase with the number of adsorbate–substrate bonds, i.e. in the sequence top $\rightarrow$ bridge $\rightarrow$ hollow. For gas-phase CO the $2\pi^\star$ LUMO is empty, and the distance between the Fermi level of the substrate and the LUMO is of decisive importance in determining the stable adsorption site (see [3] for a more detailed discussion). In gas-phase NO the $2\pi^\star$ level is occupied by a single electron and hence is pinned at the Fermi level. This facilitates $2\pi^\star$ backdonation and explains the preference for threefold coordinated adsorption on almost all surfaces. However, structural differences in the adsorption energies are small, and as discussed above, for a number of surfaces coexistence of different adsorption geometries has been reported and confirmed by the present DFT calculations. Experimentally, the adsorption geometry is characterized by the lengths of the N–O and metal–N bonds; the calculated bond lengths are compiled in figures 5 and 6, and detailed comparison of theory and experiment is given in table 4.

For on-top-adsorbed NO the calculations predict only a very modest expansion of the N–O bond length to 1.178 ± 0.004 Å, compared to 1.168 Å for the free NO molecule; the stretching of the NO bond is almost independent of the substrate. A more pronounced variation of the intramolecular bond length is predicted for bridge and hollow adsorption. For bridge-adsorbed NO, the bond length varies between $\sim$1.21 Å on Co or Ru and $\sim$1.19 Å on Pd and Au, with a more pronounced dependence on the band-filling for the 4d and 5d than for the 3d metals. The same trend is observed for adsorption in a hollow, the calculated bond lengths varying between 1.227 Å on Co and Ru and 1.194 Å on Au. The experimental values for the NO bond length are subject to considerable uncertainty: see references [1, 11, 12, 71] which report an experimental uncertainty of about ± 0.05 Å. This is about as large as the difference between the shortest N–O distance for on-top-adsorbed NO on Ni or Au, and the largest N–O distance for NO adsorbed in an hcp hollow on Co or Rh. Certain values reported in the literature, such as an N–O distance *contracted* to 1.13 Å (compared to a gas-phase value of 1.148 Å) reported for top-adsorbed NO on Rh(111) [1] or an NO bond length expanded to 1.32 Å upon adsorption

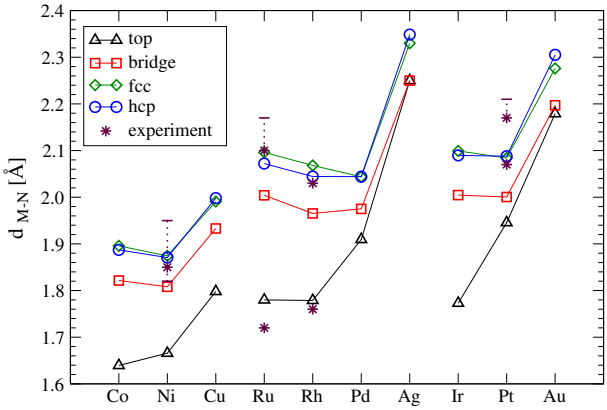

Figure 6. Trends in the calculated M–N bond length for NO adsorbed in top, bridge, fcc and hcp hollow sites on transition metal and noble metal surfaces. A line connects the metals within each row of the periodic table and stars denote experimental values taken from table 4.

Table 4. Experimental geometry of NO adsorbed on transition metals and noble metal surfaces determined by low-energy electron diffraction (LEED) or photo-electron diffraction (PED): vertical surface–nitrogen distance d_{S-N} and nitrogen–oxygen bond length d_{N-O}, compared with our calculated values characterized by the superscript 'cal'.

Surface	Site	d_{S-N} (Å)	d_{N-O} (Å)	Θ (ML)	Ref.	d^{cal}_{S-N}	d^{cal}_{N-O}
Ni(111)	Hollow	1.82 ± 0.05	1.15 ± 0.05	0.5	[11]	1.87	1.219
	fcc hollow	1.83 ± 0.07	1.17 ± 0.05	0.5	[12]	—	—
		1.83	1.17	0.25	[1]	—	—
		1.83		0.5	[13]	—	—
	hcp hollow	1.85 ± 0.07	1.18 ± 0.05	0.5	[12]	1.87	1.219
		1.95		0.5	[13]	—	—
		1.85	1.18	0.25	[1]	—	—
Cu(111)	Top	1.91 ± 0.01	—	0.33	[73]	1.795	1.181
	Bridge	—	—	—		1.930	1.206
	Hollow	—	—	—		1.985	1.218
Ru(111)	fcc hollow	2.10 ± 0.07	1.22 ± 0.06	0.75	[1, 71]	2.10	1.219
	hcp hollow	2.05 ± 0.08	1.24 ± 0.07	0.75	[1, 71]	2.07	1.226
	Hollow	—	1.32 ± 0.02		[72]	—	—
	Bridge	—	1.28 ± 0.02		[72]	2.00	1.209
	Top	1.72 ± 0.04	1.13 ± 0.06	0.75	[1, 71]	1.78	1.181
	—	—	1.20 ± 0.01		[72]		
Rh(111)	fcc hollow	2.03	1.15	0.75	[1]	2.07	1.213
	hcp hollow	2.02	1.17	0.75	[1]	2.04	1.214
	Top	1.76	1.13	0.75	[1]	1.78	1.174
Pt(111)	fcc hollow	2.17 ± 0.04	1.20 ± 0.04	0.25	[76]	2.08	1.214
	Top	2.07	1.18	0.25	[77]	1.83	1.170

in a hollow of Ru(111) [72], are simply unrealistic. Hence the comparison of the calculated NO bond lengths with the experimental values definitely does not represent a critical test of the DFT predictions. Calculations using the RPBE functional lead to essentially the same results for the structure of the adsorbate–substrate complex as the PW91 and are therefore not reported here in detail.

More reliable are the metal–N (M–N) distances derived from LEED and PED data. For NO/Ni(111) we find good agreement between theory and experiment, although our calculations cannot reproduce the difference of 0.02 Å reported for the M–N distances on adsorption in the fcc and hcp hollows [12]; but one has to note that this difference is definitely smaller than the experimental uncertainty. For NO/Cu(111), Moler *et al* [73] reported an M–N distance of 1.91 Å assigned to NO adsorbed on top in a slightly tilted configuration (tilt angle $\measuredangle$(SNO) $\sim$ 5.6°). The DFT calculations, however, predict upright adsorption in the fcc hollow, and this site preference agrees also with the interpretation of the vibrational spectroscopy [74, 75]. The experimental M–N distance also agrees reasonably well with that calculated for NO adsorbed in a hollow. For NO/Ru(0001), structural data have been reported for all four possible adsorption sites [1, 71, 72]. We note excellent agreement with the DFT calculations for NO adsorbed in one of the hollows; the calculations even faithfully reproduce the slight difference in the M–N distance for NO in the fcc and hcp hollow (see table 4). For top-adsorbed NO/Ru(0001) the M–N distance is slightly overestimated, but still close to the upper limit of the experimental estimate. For NO/Rh(111) we also find very good agreement for the M–N distances of NO in the fcc and hcp hollows and at the top site. For NO on Pt(111), where experiments [76] find the fcc hollow site to be favoured with an NO bond length of 1.20 $\pm$ 0.04 Å and a Pt–N distance 2.17 $\pm$ 0.04 Å, we note good agreement with the corresponding calculated values of $d_{\mathrm{N-O}} = 1.214$ Å and $d_{\mathrm{Pt-N}} = 2.08$ Å. For Pt(111) a coexisting on-top-adsorbed NO species has also been reported [77–79], with an M–N distance of 2.07 Å and an N–O bond length of 1.18 Å. Here theory and experiment agree very well for the N–O distance, but the experimental estimate for the M–N distance definitely seems to be too large, not only compared to the DFT results, but also in relation with the experimental results for neighbouring metals.

For some metals, a tilted adsorption geometry has been suggested and interpreted as a precursor to dissociation. Our calculational set-up admits a tilt of the NO molecule relative to the surface normal. For NO adsorbed in top sites of the Pd, Pt, Ag, and Au surfaces and also in a bridge position on Au, we find that a relatively large tilt of the adsorbed NO molecule indeed lowers the total energy. The angles between the surface normal and the molecular axis are 50° for NO adsorbed in a top site on an Au surface, 41° for Pd top and Au bridge, 49° for Pt top and 38° for Ag top. In addition to the bent geometry, the position of the N atom is not directly on top of the metal atom, but slightly shifted sideways. However, for Pd, adsorption in a top site is only metastable, with a relatively large energy difference relative to the more highly coordinated sites. On Ag and Au, the energy difference is smaller, but also in this case the tilted geometry is obtained only for metastable adsorption positions. A tilted adsorption geometry for on-top-adsorbed NO/Pt(111) has also been found in the DFT calculations of Aizawa *et al* [66], with a tilting of the N–O axis of 52° and of the Pt–N bond of 3° relative to the surface normal at a coverage of 0.25 ML, in very good agreement with our calculated tilt angles of 49° and 6°, respectively. For NO/Pt(111) a very detailed analysis of the adsorption structures using LEED has also been presented by Matsumoto *et al* [76]. For coverages of 0.5 ML and higher, models based on NO adsorption in the threefold hollow and on-top have been proposed. For on-top-adsorbed NO, the LEED fits predict a tilting of the NO molecule relative to the surface normal of about 52°–55°, in good agreement with the theoretical results.

A tilted adsorption geometry also leads to a pronounced re-hybridization of the molecular orbitals of the adsorbate and the frontier orbital of the substrate. While for an upright geometry the interaction between the d_{z^2} orbital of the metal atoms and the $2\pi^\star$ orbitals of the adsorbate is forbidden by symmetry, any tilting with respect to the surface normal induces a strong d_{z^2}–$2\pi^\star$ hybridization and an electron transfer to the antibonding $2\pi^\star$ state. The filling of the antibonding orbital leads to a further softening of the intramolecular bond, which will be

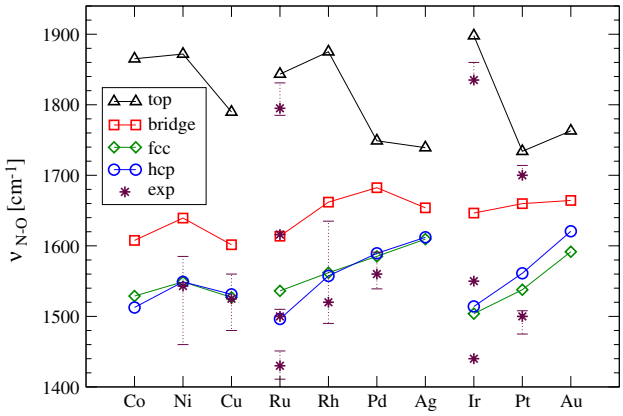

Figure 7. Calculated N–O stretching frequencies (ν_{N-O}) on close-packed transition metal and noble metal surfaces together with experimental values from table 5. Note that for on-top-adsorbed NO on Pd, Ag, Pt and Au the molecular axis is strongly tilted relative to the surface normal (see the text). The calculated ν_{N-O} for a free NO molecule is 1917 cm^{-1} and the experimental value is 1903 cm^{-1}.

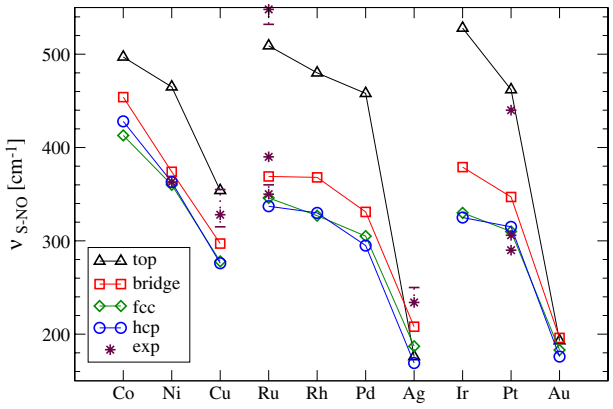

Figure 8. Calculated symmetric M–NO vibrational frequencies (ν_{M-NO}) on close-packed transition metal and noble metal surfaces, together with experimental values from table 5.

further discussed below. A tilted adsorption geometry of NO on NiO has been discussed in detail by Rohrbach *et al* [80, 81].

3.4. Vibrational frequencies

The trends in the calculated N–O stretching frequencies are summarized in figure 7, for the symmetric M–NO stretching frequencies in figure 8. Experimentally, these frequencies have been measured using reflectance-adsorption infrared spectroscopy (RAIRS), infrared adsorption spectroscopy (IRAS), (high-resolution) electron-energy-loss spectroscopy [(HR)EELS] and surface extended x-ray adsorption fine structure (SEXAFS) experiments. A detailed overview of the available experimental results is given in table 5; a condensed confrontation of theory and experiment is also contained in the graphical representations of the trends (figures 7 and 8). All vibrational frequencies have been calculated using the PW91

Table 5. Experimental and calculated symmetric metal–NO (ν_{M-CO}) and N–O (ν_{N-O}) stretching frequencies of NO adsorbed on 3d, 4d and 5d transition metal and on noble metal surfaces. The surface coverage Θ, measurement temperature, experimental technique and references to the experimental studies are also listed. RAIRS—reflection-absorption infra-red spectroscopy, (HR)EELS—(high-resolution) electron-energy-loss spectra, SFG—sum frequency generation spectroscopy. The experimental results are listed under the site assignment proposed in the respective studies, which does not always agree with the final assessment based on the combined experimental and theoretical evidence; see the text.

Surface	Site	ν_{M-NO} (cm^{-1})	ν_{N-O} (cm^{-1})	Θ (ML)	T (K)	Method	Ref.	ν^{cal}_{M-NO}	ν^{cal}_{N-O}
Co(10$\bar{1}$0)	Hollow		1443–1460		100	RAIRS	[44]	—	—
	Bridge		1643–1691		100	RAIRS	[44]	—	—
	Top		1799		100	RAIRS	[44]	—	—
Ni(111)	Hollow	363	1581	0.5	270	HREELS	[82]	363	1549
			1460–1513	Low		SEXAFS	[10]	—	—
			1543–1585	$\leqslant$0.5		SEXAFS	[10]	—	—
			1486, 1584	0.12	80	RAIRS	[83]	—	—
Cu(111)	Hollow	328	1525–1560	0–0.143	88	RAIRS	[74]	278	1527
	Bridge	315–355	1532		85	HREELS	[84]	—	—
	Top		1822		85	HREELS	[84]	—	—
			1480–1548		90	EELS	[75]	—	—
Ru(0001)	Hollow		1411–1451	0.12–0.35	150	EELS	[85]	337	1496
		360	1400		78	EELS	[86]	—	—
		350	1400–1430	0.1–0.5	115	HREELS	[87]	—	—
			1616			EELS	[78]	—	—
		680	1400			NEXAFS	[72]	—	—
	Bridge	390	1500–1510	0.2–sat	115	HREELS	[87]	368	1662
		410	1500		100	NEXAFS	[72]	—	—
	Top	532–548	1795–1831	0.35–0.82	150	EELS	[85]	480	1875
		560	1780		78	EELS	[86]	—	—
		550–560	1790–1820	0.2–sat	115	HREELS	[87]	—	—
		540	1800		100	NEXAFS	[72]	—	—
Rh(111)	Hollow	360	1480–1630	0.1 L to sat	95	EELS	[50]	330	1557
	fcc and hcp		1590	0.5			[88]	—	—
	Hollow		1520			IRAS	[89]	—	—
Pd(111)	Hollow		1539–1581	0.33		RAIRS	[90]	305	1585
			1560	Sat.		EELS	[78]	—	—
Ag(111)	Top		1855	50 L	90	RAIRS	[79]	—	—
	Top (bent/linear)	250	1750, 1879		80	HREELS	[54]	176	1739
	Top		1839	0.5 L	80	EELS	[84]	—	—
	Hollow		1258	0.5 L	80	EELS	[84]	—	—
Ir(111)	Hollow		1440			EELS	[47]	330	1503
	Bridge		1550			EELS	[47]	379	1646
	Top		1860	0.005–0.095	77–300	EELS	[47]	528	1898
	Top		1835	0–0.5	300	FT-IRAS	[91]	—	—
Pt(111)	fcc hollow	290	1490	0.25	130	HREELS	[76]	310	1538
	hcp hollow		1508	0.25	130	HREELS	[76]	315	1561
	Hollow	306					[92]	—	—
			1490		90	RAIRS	[79]	—	—
			1475–1500				[52]	—	—
			1500			EELS	[78]	—	—
			1480	Low		RAIRS	[93]	—	—
			1484			HREELS	[94]	—	—
	Top	440	1715		130	HREELS	[76]	460	1740
			1700–1714			EELS	[78]	—	—
			1700		90	RAIRS	[79]	—	—

functional only, as our work on CO has demonstrated that there are only minimal changes in the vibrational spectrum if the RPBE functional is used instead.

3.4.1. Comparison of theory and experiment. Comparison of theory and experiment is far from straightforward. For Co, Gu *et al* [44] investigated NO adsorbed on the $(10\bar{1}0)$ surface using RAIRS. Using the frequency ranges suggested by Brown and King [2], a band in the range of 1440–1460 cm^{-1} is assigned to NO in pseudo-threefold sites, the band at 1640–1700 cm^{-1} to twofold sites, and a narrow band at 1790–1800 cm^{-1} to on-top linear NO. Our frequencies calculated for the (111) surface are in accordance with this assignment, although a blue-shift of about 60 cm^{-1} for top and hollow sites suggests stronger bonding in these sites on the $(10\bar{1}0)$ than on the (111) surface, while for the twofold sites the trend is reversed.

For Ni(111), experimental measurements using different techniques, for different coverages and temperatures, are available [10, 82, 83]. The stretching frequency of NO on Ni(111) is measured at 1486 cm^{-1} at 80 K and an initial exposure to 0.5 L NO. Irradiation of the NO layer on the Ni(111) surface dissociates part of molecules and an additional peak appears at ∼1835–1881 cm^{-1}) in the vibrational spectra [83]. After full irradiation a clean surface is expected, but after 3 L NO exposure to achieve saturation coverage two peaks appear at 1563 and 1865 cm^{-1}. Hence, atomic and molecular species need not be visible on the surface after complete irradiation of the surface. Additionally, increasing the temperature to 300 K parallel to a higher NO exposure (from 3 to 50 L) is necessary to achieve saturation coverage. Under irradiation at 300 K, two bands at 1870–1880 cm^{-1} and at 1613 cm^{-1} are detected in the RAIRS spectra [83]. The low-frequency band centred around ∼1550 cm^{-1} agrees very well with our result for hollow-adsorbed NO. This is in accordance with the site assignment based on photoelectron diffraction [12] and photoemission [13] experiments, but disagrees with earlier assignments [10, 15] to tilted and linear bridge-bonded NO. The coverage dependence results from lateral interactions. The calculated M–NO stretching frequency is in excellent agreement with the HREELS result of Stirniman *et al* [82]. The high-frequency bands observed after irradiation agree very well with the NO stretching frequencies for bridge-bonded and on-top-bonded NO. Atomic N and O formed on dissociation bind very strongly to the substrate, blocking the more favourable hollow sites and pushing molecular NO towards the less stable sites.

For NO on Cu(111), So *et al* [54] reported on the basis of HREELS experiments the existence of two vibrational bands at saturation coverage, assigned to on-top-bonded and bridge-bonded species. Dumas *et al* [74] and Wendelken [75] on the other hand claimed that up to a monolayer coverage, only adsorption in a threefold hollow and in an upright geometry is observed. The NO stretching frequency is slightly upshifted with increasing coverage. Our calculated molecular stretching frequency for hollow adsorption is in excellent agreement with the experimental values and clearly contradicts an assignment of the 1532 cm^{-1} mode to bridge-bonded NO. The high-frequency mode reported by So *et al* (1822 cm^{-1}) lies about 30 cm^{-1} above our calculated frequency for on-top-adsorbed NO.

A wealth of experimental data is available for NO on Ru(0001) [62, 72, 85–88, 90]. Both N–O and M–NO stretching frequencies have been identified for adsorption in all three high-symmetry sites, in agreement with the small site-dependent differences in the adsorption energies (see figure 2). All N–O stretching frequencies show a considerable variation with coverage and temperature, frequencies assigned to hollow and bridge sites overlap. As the most stable adsorption sites, our calculations have identified the hcp hollow. The corresponding calculated N–O mode lies at the upper edge of the range covered by the experimental data, and for the bridge and hollow sites we also overestimate the N–O stretching frequency. On the other hand, the calculated M–NO stretching frequencies are always softer than the experimental

values. This suggests that the bonding of the molecule to the substrate is too soft, while the smaller red-shift of the calculated frequencies indicates a weaker activation of the molecule. However, it has to be admitted that the anharmonicity of the stretching frequencies plays a certain role. It was already shown that anharmonic effects shift the N–O stretching frequency to slightly lower values [18], reducing the differences between theory and experiment.

For Rh, Pd and Ir extensive DFT investigations of the vibrational frequencies of NO adsorbed on the (111) surface have been performed by Loffreda *et al* [18] and Krekelberg *et al* [21], both using ultrasoft pseudopotentials. The harmonic(anharmonic) frequencies for NO/Rh(111) reported by Loffreda *et al* are 1882(1812)/1677(1644)/1629(1544)/1622(1554) cm^{-1} for top/bridge/hcp/fcc at a coverage of 0.33 ML; increasing the coverage to 0.5 ML upshifts the frequencies by about 25 and 40 cm^{-1} for bridge and hollow sites, respectively. Our harmonic frequencies for 0.25 ML coverage calculated using the all-electron PAW approach are 1875/1662/1563/1557 cm^{-1} (in the same sequence). The differences in the harmonic frequencies are modest for top and bridge sites and substantially larger for the hollow sites. Similar differences are encountered for NO/Pd(111): using US-PP Loffreda *et al* calculate harmonic(anharmonic) frequencies of 1865(1812)/1693(1667)/1627(1588)/1618(1574) cm^{-1} for top/bridge/hcp/fcc; we find using PAW harmonic frequencies of 1683/1588/1592 cm^{-1} for bridge/hcp/fcc. Hence the slightly more accurate PAW calculations yield systematically lower NO stretching frequencies, the difference being larger for highly coordinated adsorption sites. Experimentally, EELS measurements on NO/Rh(111) by Root *et al* [50] yield an NO stretching frequency for NO adsorbed in a hollow increasing from 1480 cm^{-1} at very low exposures ($\leqslant$0.1 L) to 1630 cm^{-1} at saturation, and a low-intensity mode at 1840 cm^{-1} assigned to on-top-adsorbed NO at saturation coverages. In contrast, only one mode at 1520 cm^{-1} assigned to hollow-adsorbed NO has been reported in the IRAS measurements of Weaver *et al* [89]. For NO/Pd(111) coverage-dependent NO-stretching frequencies ranging from 1539 to 1581 cm^{-1} have been reported [62, 89, 90]. Hence for both metals we find good agreement of the low-coverage measurements with our results, with a small margin for improvement by anharmonic corrections.

Our result for on-top-adsorbed NO on the (111) surfaces of Pd, Pt, Ag and Au deserves special comment. As emphasized above, NO adsorbed on the top sites of these metals is unstable in an upright position and shows a large tilt relative to the surface normal. Our NO-stretching frequencies calculated for top-adsorbed NO on these metals are calculated for this tilted configuration; this explains the anomalous softening of the NO-stretching modes displayed in figure 7.

Krekelberg *et al* [21] calculated the stretching frequencies of NO on an Ir(111) surface using a pseudopotential approach. Their calculated NO eigenfrequencies are 1924 cm^{-1} for top sites, 1669 cm^{-1} for bridge and 1536 cm^{-1} for hcp hollow sites. Again our stretching frequencies from an all-electron PAW approach (top—1898 cm^{-1}, bridge—1646 cm^{-1}, fcc hollow—1503 cm^{-1}, hcp hollow—1514 cm^{-1}) are lower, with a systematic down-shift of about 25 meV. Smaller differences are observed for the surface–NO stretching frequencies: top—525(528) cm^{-1}, bridge—364(379) cm^{-1}, hcp hollow 337(325) cm^{-1} (present results in parentheses). This shows that the difference between the pseudopotential and all-electron calculations is larger for the intramolecular stretching frequencies depending on the strongly non-local pseudopotentials of N and O, than for the surface–adsorbate interactions. The EELS experiments of Davis *et al* [47] have identified loss features at three different frequencies. At very low exposure at low temperatures, only a single mode at 1860 cm^{-1} assigned to on-top-adsorbed NO is observed. Increasing coverages show an additional feature at 1550 cm^{-1} and with further increases a feature at 1440 cm^{-1}. The intensity ratio of theses two loss

features is $I_{1550}/I_{1860} \sim 0.35$–$0.50$ after exposure to a molecular beam with a kinetic energy of 1.3 eV, it decreases to 0.2 for the highest coverage reached with a low-energy beam of only 0.056 eV. The intensity of the 1440 cm^{-1} remains very low at all coverages. On the basis of our detailed analysis of the PES for NO/Ir(111) we have argued that the three loss features registered in EELS should be assigned to top-, bridge-, and hollow-adsorbed NO. This assignment is certainly strongly supported by the good agreement between calculated and measured frequencies (allowing for slightly larger anharmonic corrections due to the flat PES) and by the fact that the intensity of the modes decreases with decreasing adsorption energy. Interestingly, the co-adsorption study of NO and CO on Ir(111) by Tang *et al* [91] has identified (using IRAS) only the high-frequency NO mode, even at much higher coverages.

For NO/Pt(111), the EELS and RAIRS experiments of Matsumoto *et al* [76, 94], combined with structural analyses based on LEED, produced three stretching modes at 1490, 1508, and 1715 cm^{-1} assigned to NO in the fcc, hcp and top sites, in good agreement with our calculated eigenmodes and with the previous calculations of Aizawa *et al* [66]. The anomalously low stretch frequency for on-top adsorption is a consequence of the tilted adsorption geometry. Reasonable agreement is also achieved for the substrate–adsorbate stretch modes. The frequencies for hollow-adsorbed molecules reported by Matsumoto *et al* are also in good agreement with a number of other experimental studies; see table 5 for details.

NO/Ag(111) forms a highly mobile species, as confirmed by the small energy differences for adsorption in different high-symmetry sites. Because of this high mobility, NO molecules can approach each other very easily, forming $(NO)_2$ dimers, or react to form N_2O [54, 79, 84, 95]. The coexistence of different adsorbed species, and of linear and bent adsorption geometries, considerably complicates the interpretation of the measured vibrational spectra. So *et al* [54, 84] assigned a high-frequency mode at 1839 cm^{-1} to NO adsorbed in a linear on-top position, while a lower frequency at 1750 cm^{-1} was assigned to a bent on-top position. Low-frequency modes at 1258 and 1153 cm^{-1} were assigned to linear and bent 'threefold bridge' (probably meaning hollow) sites. Brown *et al* [95] reported a single band at 1865 cm^{-1} at the lowest exposures, and further bands at 1776 and 1789 cm^{-1} at slightly larger exposures, assigned on the basis of NEXAFS studies to NO dimers in different adsorption geometries. A band at 1260 cm^{-1} appearing on heating above 70 K was attributed to adsorbed N_2O. Our calculations find an upright on-top adsorption to be unstable, and a stretching frequency of 1739 cm^{-1} for a bent on-top geometry, in reasonable agreement with the mode measured by So *et al*. For this geometry we also find a very soft Ag–NO stretching mode. The modes with frequencies larger than 1800 cm^{-1} assigned to a linear on-top geometry are probably due to the stretching modes of NO dimers, as suggested by Brown *et al*. For bridge- and hollow-adsorbed NO we calculate frequencies close to 1600 cm^{-1}, i.e. quite far for the modes assigned to a highly coordinated adsorption geometry. The low-frequency modes reported by So *et al* are therefore to be assigned to reaction products of NO. No experimental studies of the vibrational properties of NO/Au(111) are known; our studies suggest a similar scenario to that on Ag surfaces.

Altogether, our results allow us to complete the trends suspected on the basis of the experimental data: for NO adsorbed in hollow positions on the surfaces of 3d metals or Cu, we find only a small variation of the stretching frequency with the d-band filling. This is in contrast to the strong increase found for NO on the surfaces of the 4d and 5d metals and on Ag and Au; it is interesting that the stretching frequencies show a much more pronounced variation than the adsorption energies. The M–NO stretching frequencies follow this trend much more closely, the reduced adsorption strength resulting directly in a softer M–NO mode. A much weaker dependence on the band filling is noted for bridge-adsorbed NO. The N–O stretching frequencies for on-top-adsorbed NO show a quite anomalous variation: the softening observed

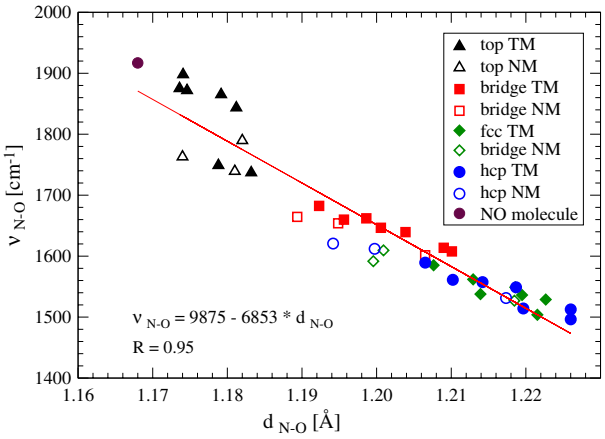

Figure 9. Correlation between the calculated N–O bond length ($d_{N–O}$) and the N–O stretching frequency ($\nu_{N–O}$) for all high-symmetry on-surface sites. TM—transition metals, NM—noble metals. A free molecule with $d_{N–O} = 1.168$ Å and $\nu_{C–O} = 1917$ cm^{-1} is also considered.

on the noble metal surfaces and on Pd and Pt resulting from the tilted adsorption geometries. For the M–NO stretching frequencies we find a pronounced softening with increased d-band filling. The softening is particularly pronounced for the heavy noble metals Ag and Au, in agreement with a weak chemisorption on these surfaces.

3.4.2. Site assignment based on vibrational spectroscopy. We can establish new ranges of the N–O stretching frequencies which correspond to the coordination of the adsorption site. The intervals are 1490–1620 cm^{-1} for threefold coordinated hollow site, 1600–1690 cm^{-1} for bridge site and 1730–1900 cm^{-1} for top-bonded sites. Compared to the frequency ranges proposed by Perez-Jigato *et al* [32] on the basis of cluster calculations (see the introduction) we note a very reasonable agreement. There is only a very small overlap between the stretching frequencies of NO in bridge and hollow sites and no overlap between the top and bridge sites. However, one should be especially careful close to the borders of intervals if using the intervals to deduce the adsorption sites. For the metal–adsorbate stretching mode, a strong difference in the eigenfrequencies is found only between on-top and bridge or hollow adsorption on the transition metals. For the noble metals, only very small site-dependent frequency shifts are calculated.

3.4.3. Correlations between adsorption geometry and vibrational eigenmodes. The correlation between the adsorption geometry (site, NO bond length, and metal–adsorbate distance) and the vibrational modes is analysed in figures 9 and10. The correlation between the N–O bond length $d_{N–O}$ and $\nu_{N–O}$ is roughly linear, but considerable scatter is found for on-top-adsorbed NO. The tilted NO adsorbates on Pd, Pt, Ag and Au have distinctly softer NO-stretching modes, albeit without an elongation of the bond length, i.e. the softening of the eigenmode does not necessarily induce at the same time an activation for dissociation. For NO adsorbed in bridge and hollow sites, the calculated NO bond lengths show a much stronger overlap than the eigenfrequencies. Fitting the frequencies belonging to the bridge and hollow sites separately by a straight line leads to a smaller variation of the frequency with the bond length. The slope remains the same for both bridge- and hollow-adsorbed NO, with an upshift of about 40 cm^{-1} for bridge-bonded NO.

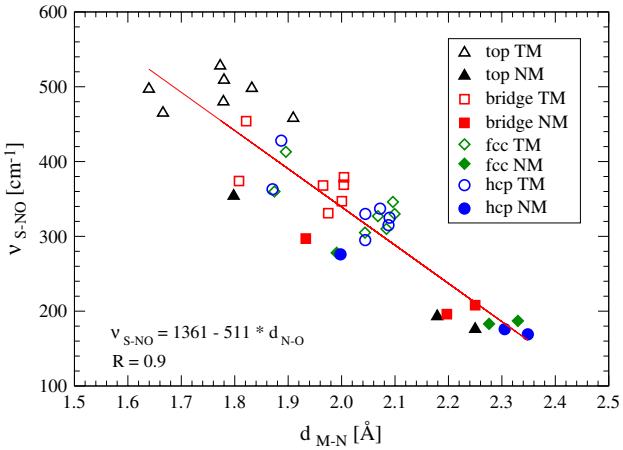

Figure 10. Correlation between the calculated M–N distance ($d_{\mathrm{M-N}}$) and the S(urface)–NO stretching frequency ($\nu_{\mathrm{S-NO}}$) for all high-symmetry on-surface sites on transition (TM) and noble (NM) metals.

The correlation between the metal–nitrogen distance and the surface–NO (S–NO) stretching frequency demonstrates the particular character of NO adsorption on Ag and Au: irrespective of the adsorption sites we find a large metal–adsorbate distance and a very soft stretching mode. For the transition metals and Cu, the distance–frequency correlation is roughly linear. The shortest surface–adsorbate distances and the hardest S–NO stretching modes are found for on-top-adsorbed NO, with the shortest distances found for the ferromagnetic 3d metals Co and Ni. Also, for the more highly coordinated sites, these metals allow for a shorter approach of the molecule, leading via an increased Pauli repulsion to a stiffer S–NO mode. All 4d and 5d metals cluster in a narrow region: within these groups the variation of the S–NO stretching frequency is not determined by the metal–adsorbate distance, but by the decreasing adsorption strength with increasing band filling.

4. Discussion and conclusions

The molecular adsorption of NO on the close-packed surfaces of transition and noble metal surfaces has been investigated using state-of-the-art *ab initio* DFT techniques. To rationalize the trends across this group of metals we have explored the site preference of the adsorbed molecule, calculated the adsorption energies, the adsorption geometries and the vibrational properties of the adsorbate–substrate complex. Detailed comparisons with the available experimental data and with earlier theoretical studies are presented.

For all metals—except Ir and Au—theory predicts a preference for adsorption in a hollow site with a threefold coordination of the adsorbate by metal atoms. On Ir(111) only minimal site-dependent differences in the adsorption energies are found, with a slight preference for linear on-top adsorption. On Au(111), where NO adsorption is only very weak, bridge adsorption with a strong tilting of the NO molecule relative to the surface normal is predicted. Among the two different hollow sites on a (111) surface, preference changes from hcp on Co, Ni, Ru, Rh to fcc on Cu, Pd, Ag and Pt. However, not only on Ir, but also on Co, Ru, Rh, and Pt, are the site-dependent differences in the adsorption energies small enough to allow a simultaneous occupation of different sites. The predicted site preferences agree with the

revised experimental assignments and with all other state-of-the-art DFT calculations. It is also important to note that the predicted site preference is independent of the choice of the exchange–correlation functional.

This is not the case for the absolute values of the adsorption energies: the RPBE functional leads consistently to adsorption energies lower by about 0.5 eV/atom than the PW91 functional (which yields, however, a slightly more accurate description of the clean surfaces; see [3]). For the transition metal surfaces the reduction of the adsorption energies improves agreement with experiment, although reliable experimental data are scarce and care must be exercised in comparing the calculated *integrated* adsorption energies with the *differential* adsorption energies derived from TPD spectra. There is also a considerable scatter among the available theoretical results, to be attributed to different choices of pseudopotentials, basis-set sizes and Brillouin zone integration meshes. We are confident that our results are well converged: the benefit of the increased computational effort is that systematic trends in the calculated adsorption energies and other physical properties can be explored. For the noble metal surfaces the strong reduction of the adsorption energies resulting from the use of the RPBE functional leads to poor agreement with experiment, especially for Ag and Au where NO is predicted to be unbound to the surface. For this reason, the analysis of the vibrational spectra was based on the PW91 functional only.

The comparison of the calculated bond lengths of the adsorbed molecule and of the surface–adsorbate distances with experiment is hampered by uncertainties in the experimental values which often exceed the variation across the entire series of substrates. A critical analysis, however, leads to very encouraging conclusions.

For the analysis of the vibrational properties, again a careful confrontation of theory and experiment leading in several cases to a revision of the original assignment of the observed vibrational modes, is required. If this is done, a very nice agreement of the predicted trends in the vibrational frequencies with experiment is achieved. Our comprehensive set of results also allows one to define the frequency ranges associated with the different adsorption geometries: the revised site assignment only leads to the agreement between theory and experiment noted above.

In the introduction we have addressed the characteristic differences in the adsorption properties of NO and CO. The first is the tendency to an occupation of top sites by CO on the surfaces of the noble metals and on Pt, Rh, Ir and Ru, while the adsorbed NO is threefold coordinated with the only exceptions of Ir and Au. While a correct site prediction is a serious problem for CO (where the hollow site remains preferred in DFT calculations also for Rh, Pt and Cu) and can be cured only via post-DFT corrections improving the calculated HOMO–LUMO gap of the molecule (see [3]), no such problem exists for NO. Even the difficult case of NO/Ir(111) is correctly predicted by DFT, as demonstrated by the analysis of the vibrational spectrum. The reason is that the fractionally occupied $2\pi^\star$ orbital is always pinned at the Fermi level. Another difference is that for CO on 3d and 4d transition metal surfaces the calculated adsorption strength increases with the d-band filling, and hence with a decreasing distance of the d-band centre from the Fermi edge, in general agreement with the d-band model proposed by Hammer and Nørskov [96, 97]. For NO, on the other hand, the calculated adsorption energy shows only little variation with the d-band filling, and a decrease rather than an increase for 3d, 4d, and 5d metals as well. Hence for NO the d-band model could explain the much weaker adsorption of NO on the noble than on the transition metals, but not the variation within the transition metal series. A detailed discussion of adsorption in terms of the hybridization of the fully occupied 1π and 5σ orbitals and of the empty $2\pi^\star$ orbital with the d-states of the substrate has been given in [3]. For CO, the $2\pi^\star$ orbital is empty and the 5σ and 1π orbitals are located about 7 and 9.5 eV below the LUMO. Upon adsorption, the 5σ state is shifted

below the 1π state which hybridizes strongly with the lower d-band (see figure 10 in [3]). However, all interactions of the 1π orbital with d-states are located below the Fermi level and have purely repulsive character. Adsorbate–substrate bonding is promoted primarily by electron donation from the 5σ state, while back-donation from the d_π states of the substrate to the antibonding $2\pi^\star$ molecular orbital contributes to the reduction of the intramolecular bond strength. The same mechanisms also dominate the adsorption of NO, but now the partially filled $2\pi^\star$ orbital is pinned at the Fermi edge, and the 5σ and 1π orbital are located at higher binding energies. Hence the repulsive interactions arising from the interaction of the 1π state with the d-band are greatly reduced, while donation from the 5σ state is still efficient; this explains the larger adsorption energy of NO compared to CO (although it must be admitted that an experimental confirmation of this trend is still missing). Backdonation to the $2\pi^\star$ states leads to an increased occupation and a reduction of the magnetic moment of the adsorbed molecule; on most metals adsorbed NO is even completely demagnetized. The increased $2\pi^\star$ occupancy also correlates with the preference for the highly coordinated hollow site, and with the red-shifts of the NO-stretching modes. For NO adsorbed in on-top sites, the interaction is mainly with the d_{z^2} orbitals extending farthest from the surface, while the d_π–$2\pi^\star$ interaction is weak (and hence there is almost no backdonation), leading to a modest red-shift only. d_π–$2\pi^\star$ interaction and back-donation increase on moving to bridge and hollow sites, causing a much more pronounced softening of the NO stretch-mode. With increasing band filling, the centre of the d-band moves to higher binding energies, causing a reduced backdonation and hence a smaller red-shift of the NO vibrations (see figure 7).

For NO in a top or bridge position on the heavy noble metals Ag and Au and on Pd and Pt, the d_π–$2\pi^\star$ interaction is too weak to stabilize this adsorption geometry. In these cases, a tilted position allows for a strong d_{z^2}–$2\pi^\star$ hybridization and a bonding to the substrate which is as strong as on the threefold coordinated sites.

In conclusion, a comprehensive DFT investigation of the adsorption of molecular NO on close-packed surfaces of late transition metals and noble metals has been performed. The results elucidate clear trends in the variation of the adsorption energy, and in the structure and vibrational properties of the adsorbate–substrate complex. A careful comparison with the available experimental data has been performed. For the vibrational eigenmodes we find good agreement between theory and experiment: in those cases where the original site assignment was been revised as a result of the DFT calculations, this is usually supported by structural investigations based on LEED or STM. Considerable disagreement subsists between the calculated and measured adsorption energies, both in their absolute values and in the trends across the series. For the transition metal surfaces the prediction of too large adsorption energies can partially be corrected by replacing the PW91 GGA functional by the RPBE functional, but the trends remain the same. For the noble metal surfaces, the RPBE corrections definitely overshoot. In any case supplementary experimental information would be very valuable for a critical assessment of the accuracy of the DFT predictions. The adsorption energies for molecular NO are also important for the dissociation catalysed by the metallic substrate. DFT studies of NO dissociation will be reported in a forthcoming publication.

References

[1] Over H 2001 *Prog. Surf. Sci.* **58** 249
[2] Brown W A and King D A 2000 *J. Phys. Chem.* B **104** 2578
[3] Gajdoš M, Eichler A and Hafner J 2004 *J. Phys.: Condens. Matter* **16** 1141
[4] Huber K and Herzberg G 1979 *Mol. Spectra Diatomic Mol.* **77** 2008
[5] Cuthill M A, Fabian D J and Shu-Shou-Shen 1973 *J. Phys. Chem.* **77** 2008

[6] Brodén G, Rhodin T, Bruckner C, Benbow R and Hurych Z 1976 *Surf. Sci.* **59** 593
[7] Canning N D S and Madix R J 1984 *J. Phys. Chem.* **88** 2431
[8] Muetterties E L and Wexler R M 1983 *Surv. Prog. Chem.* **10** 61
[9] Netzer F P and Madey T E 1981 *Surf. Sci.* **110** 251
[10] Erley W 1988 *Surf. Sci.* **205** L771
[11] Aminpirooz S, Schmalz A, Becker L and Haase J 1992 *Phys. Rev.* B **45** 6337
[12] Lindsay R, Theobald A, Giessel T, Schaff O, Bradshaw A M, Both N A and Woodruff D P 1998 *Surf. Sci.* **405** L566
[13] Asensio M C, Woodruff D P, Robinson A W, Schindler K-M, Gardner P, Ricken D, Bradshaw A M, Conesa J C and González-Elipe A R 1992 *J. Vac. Sci. Technol.* A **10** 2445
[14] Mapledoram L D, Winder A and King D A 1993 *Chem. Phys. Lett.* **208** 409
[15] Lehwald S, Yates J T and Ibach H 1980 *Proc. IVC-8, ISS-4, ECOSS-3 (Cannes, 1980)* ed D A Degras and M Costa, p 221
[16] Neyman K M and Rösch N 1994 *Surf. Sci.* **307–309** 1193
[17] Ge Q and King D A 1998 *Chem. Phys. Lett.* **285** 15
[18] Loffreda D, Simon D and Sautet P 1998 *Chem. Phys. Lett.* **291** 15
[19] Loffreda D, Simon D and Sautet P 2003 *J. Catal.* **213** 211
[20] Mavrikakis M, Rempel J, Greeley J, Hansen L B and Nørskov J K 2002 *J. Chem. Phys.* **117** 6737
[21] Krekelberg W P, Greeley J and Mavrikakis M 2004 *J. Phys. Chem.* B **108** 987
[22] Ge Q, Brown W A, Sharma R K and King D A 1999 *J. Chem. Phys.* **110** 12082
[23] Eichler A and Hafner J 2001 *Chem. Phys. Lett.* **343** 383
[24] Eichler A and Hafner J 2001 *J. Catal.* **204** 118
[25] Mannstadt W and Freeman A J 1997 *Phys. Rev.* B **55** 13298
[26] Bogicevic A and Hass K C 2002 *Surf. Sci.* **506** L237
[27] Hammer B 1999 *Phys. Rev. Lett.* **83** 3681
[28] Delbecq F and Sautet P 1999 *Surf. Sci.* **442** 338
[29] Hass K C, Tsai M H and Kasowski R V 1996 *Phys. Rev.* B **53** 44
[30] Ge Q, Jenkins S J and King D A 2000 *Chem. Phys. Lett.* **327** 125
[31] Spišák D and Hafner J 2001 *Phys. Rev.* B **64** 094418
[32] Peréz-Jigato M, Somasundram K, Termath V, Handy N C and King D A 1997 *Surf. Sci.* **380** 83
[33] Endou A, Ohashi N, Yoshizawa K, Takami S, Kubo M, Miyamoto A and Broclawik E 2000 *J. Phys. Chem.* B **104** 5110
[34] Kresse G and Furthmüller J 1996 *Phys. Rev.* B **54** 11169
[35] Kresse G and Joubert D 1999 *Phys. Rev.* B **59** 1758
[36] Blöchl P 1994 *Phys. Rev.* B **50** 17953
[37] Perdew J P and Zunger A 1981 *Phys. Rev.* B **23** 5048
[38] Perdew J P, Chevary J A, Vosko S H, Jackson K A, Pederson M R, Singh D J and Fiolhais C 1992 *Phys. Rev.* B **46** 6671
[39] Hammer B, Hansen L B and Nørskov J K 1999 *Phys. Rev.* B **59** 7413
[40] Kresse G, Gil A and Sautet P 2003 *Phys. Rev.* B **68** 073401
[41] Gajdos M and Hafner J 2005 *Surf. Sci.* **590** 117
[42] Gajdos M, Eichler A, Hafner J, Meyer G and Rieder K H 2005 *Phys. Rev.* B **71** 035402
[43] Press W, Teukolsky S, Vetterling W and Flannery B 2002 *Numerical Recipies in C++* (New York: Cambridge University Press)
[44] Gu J, Yeo Y Y, Mao L and King D A 2000 *Surf. Sci.* **464** 68
[45] Nakamoto K 1986 *Infrared and Raman Spectra of Inorganic and Coordination Compounds* 4th edn (New York: Wiley)
[46] Zhang Y and Yang W 1997 *Phys. Rev. Lett.* **80** 890
[47] Davis J E, Karseboom S G, Nolan P D and Mullins C B 1996 *J. Chem. Phys.* **105** 8362
[48] Hansen K H, Šljivančanin Ž, Hammer B, Lægsgaard E and Stensgaard F B I 2002 *Surf. Sci.* **496** 1
[49] Wartnaby C E, Stuck A, Yeo Y Y and King D A 1996 *J. Phys. Chem.* **100** 12483
[50] Root T W, Fisher G B and Schmidt L D 1988 *J. Chem. Phys.* **85** 4679
[51] Zhdanov V P and Kasemo B 1996 *Catal. Lett.* **40** 197
[52] Borg H J, Reijerse J-J, van Santen R A and Niemantsverdriet J W 1994 *J. Chem. Phys.* **101** 10052
[53] Ramsier R D, Gao H N Q, Lee K W, Nooij O W, Lefferts L and Yates J T Jr 1994 *Surf. Sci.* **320** 209
[54] So S K, Franchy R and Ho W 1989 *J. Chem. Phys.* **91** 5701
[55] Gorte R J and Schmidt L D 1981 *Surf. Sci.* **109** 367
[56] Campbell C T, Ertl G and Segner J 1982 *Surf. Sci.* **115** 309

[57] Serri J A, Tully J C and Cardillo M J 1983 *J. Chem. Phys.* **79** 1530
[58] Mummey M J and Schmidt L D 1981 *Surf. Sci.* **109** 29
[59] Eichler A, Kresse G and Hafner J 1996 *Phys. Rev. Lett.* **77** 1119
[60] Eichler A, Kresse G and Hafner J 1997 *Surf. Sci.* **397** 116
[61] Hammer B 2000 *Surf. Sci.* **459** 323
[62] Koper M T M, van Santen R A, Wasileski S A and Weaver M J 2000 *J. Chem. Phys.* **113** 4392
[63] Hermse C G M, Frechard F, van Bavel A P, Lukkien J J, Niemantsverdriet J W, van Santen R A and Jansen A P J 2003 *J. Chem. Phys.* **118** 7081
[64] Loffreda D, Simon D and Sautet P 1998 *J. Chem. Phys.* **108** 6447
[65] Honkala K, Pirilä P and Laasonen K 2001 *Phys. Rev. Lett.* **86** 5942
[66] Aizawa H, Morikawa Y, Tsuneyuki S, Fukutani K and Ohno T 2002 *Surf. Sci.* **514** 394
[67] Gil A, Clotet A, Ricart J M, Kresse G, García-Hernández M, Rösch N and Sautet P 2003 *Surf. Sci.* **530** 71
[68] Feigerle C, Seiler A, Pena J, Celotta R and Pierce D 1986 *Phys. Rev. Lett.* **56** 2207
[69] Spisak D and Hafner J 2001 *Phys. Rev.* B **64** 094418
[70] Stibor A, Kresse G, Eichler A and Hafner J 2002 *Surf. Sci.* **507–510** 99
[71] Stichler M and Menzel D 1997 *Surf. Sci.* **391** 47
[72] Esch F, Ladas S, Kennou S, Siokou A and Imbihl R 1996 *Surf. Sci.* **355** L253
[73] Moler E J, Kellar S A, Huff W R A and Hussain Z 1996 *Phys. Rev.* B **54** 10862
[74] Dumas P, Suhren M, Chabal Y J, Hirschmugl C J and Williams G P 1997 *Surf. Sci.* **371** 200
[75] Wendelken J F 1982 *J. Vac. Sci. Technol.* **20** 884
[76] Matsumoto M, Tatsumi N, Fukutani K and Okano T 2002 *Surf. Sci.* **513** 485
[77] Materer N, Barbieri A, Gardin D, Starke U, Batteas J D, Van Hove M A and Somorjai G A 1993 *Phys. Rev.* B **48** 2859
[78] Koper M T, van Santen R A, Wasileski S A and Weaver M J 2000 *J. Chem. Phys.* **113** 4392
[79] Itoyama T, Wilde M, Matsumoto M, Okano T and Fukutani K 2001 *Surf. Sci.* **493** 84
[80] Rohrbach A, Hafner J and Kresse G 2004 *Phys. Rev.* B **69** 075413
[81] Rohrbach A and Hafner J 2005 *Phys. Rev.* B **71** 045405
[82] Stirniman M J, Li W and Sibener S J 1994 *J. Chem. Phys.* **102** 4699
[83] Magkoev T T, Song M-B, Fukutani K and Murata Y 1996 *Surf. Sci.* **363** 281
[84] So S K, Franchy R and Ho W 1991 *J. Chem. Phys.* **95** 1385
[85] Thomas G E and Wienberg W H 1978 *Phys. Rev. Lett.* **41** 1181
[86] Schwalke U and Weinberg W H 1987 *J. Vac. Sci. Technol.* A **5** 459
[87] Neyman K M, Rösch N, Kostov K L, Jacob P and Menzel D 1994 *J. Chem. Phys.* **100** 2310
[88] Kao C T, Blackman G S, van Hove M A, Somorjai G A and Chan C-M 1989 *Surf. Sci.* **224** 77
[89] Weaver M J, Zou S and Tang C 1999 *J. Chem. Phys.* **111** 368
[90] Nakamura I, Fujitani T and Hamada H 2002 *Surf. Sci.* **514** 409
[91] Tang C, Zou S, Severson M W and Weaver M J 1998 *J. Phys. Chem.* B **102** 8546
[92] Hayden B 1983 *Surf. Sci.* **131** 419
[93] Severson M W and Overend J 1982 *J. Chem. Phys.* **76** 1584
[94] Matsumoto M, Fukutani K, Okano T, Miyake K, Shigekawa H, Kato H, Okuyama H and Kawai M 2000 *Surf. Sci.* **454–456** 101
[95] Brown W A, Gardner P, Perez Jigato M and King D A 1995 *J. Chem. Phys.* **102** 7277
[96] Hammer B and Nørskov B 2000 *Adv. Catal.* **45** 71
[97] Nørskov J K 1990 *Rep. Prog. Phys.* **53** 1253
[98] http://cms.mpi.univie.ac.at/vasp/
[99] Hammer B, Hansen L and Nørskov J 1999 *Phys. Rev.* B **59** 7413
[100] Payne M, Teter D A M P, Arias T and Joannopoulos J 1992 *Rev. Mod. Phys.* **64** 1045
[101] Laasonen K, Pasquarello A, Car R, Lee C and Vanderbilt D 1993 *Phys. Rev.* B **47** 10142
[102] Morikawa Y 2001 *Phys. Rev.* B **63** 033405
[103] te Velde G and Baerends E 1991 *Phys. Rev.* B **44** 7888